2014 IEEE International Conference on Robotics & Automation (ICRA)
Hong Kong Convention and Exhibition Center
May 31 - June 7, 2014. Hong Kong, China

Area Coverage Planning that Accounts for Pose Uncertainty with an AUV Seabed Surveying Application

Liam Paull[1], Mae Seto[2] and Howard Li[3]

***Abstract*— This paper presents an overview of our research on accounting for robot pose uncertainty in area coverage applications. In the vast majority of existing literature on robotics area coverage, the location uncertainty of the robot is not considered. An uncertain robot pose results in an uncertain sensor swath, which in turn creates uncertainty about the achieved coverage. Here, we present a general framework where pose estimates are mapped through the coverage sensor model to obtain a probability of coverage over the discretized workspace. This probabilistic representation can then be used to adaptively plan paths for coverage based on an entropy reduction formulation.**

This framework is particularly well-suited to autonomous underwater vehicles (AUVs) performing seabed surveying operations. The AUV position estimate diverges from the actual AUV position while submerged due to the lack of a global position reference. This discrepancy can result in parts of the seabed being missed, which is unacceptable in safety-critical missions such as mine countermeasures. The proposed information-based path planning approach is able to guarantee area coverage even in the case of severe AUV position estimate drift. In-water experiments with an AUV show the effectiveness of the method.

I. Introduction

Coverage of an area is a common task for a robotic platform and has many applications. Different methods for generating provably complete coverage paths exist in the literature [1], [2]. However, as is noted in [3] "The term complete is used in the motion planning sense, not in the operating research field sense." While a deterministic planner might produce complete coverage plans there is no guarantee of actual area coverage in the field.

Seabed surveying by an autonomous underwater vehicle (AUV) can be considered as an area coverage problem [4]. With the reduction in size and cost of AUVs, this mission is now being completely automated. Localization of an AUV when submerged without the use of pre-localized beacon hardware is a challenging task [5]. In this work we extend the capabilities of these low-cost vehicles with relatively poor navigation to safety-critical missions such as seabed surveying for mine countermeasures (MCM)

As motivation, consider Fig. 1 which shows a real AUV attempting to cover (scan) an area of seabed with a sidescan sonar (SSS). The mission was run on the surface for access to GPS for ground truth but the GPS measurements are not fused to generate the state estimate when the AUV is within the workspace (yellow box). This simulates the AUV submerging to perform the survey and then surfacing at the end of each leg for a GPS fix. AUV position was estimated on-board using an extended Kalman filter (EKF) which fused velocity over ground measurements from the Doppler velocity log (DVL) and heading from the compass. Fig. 1-a shows the workspace (region to scan) in yellow, the pre-planned lawn mower style tracks to scan the area with the SSS in green, the AUV position estimates from the EKF in red, and the actual trajectory from the GPS data in blue. Fig. 1-b shows the desired coverage that would be achieved if the AUV were able to exactly follow its pre-planned lawn mower tracks, Fig. 1-c shows the believed coverage based on the EKF position estimates, and Fig. 1-d shows the coverage based on the GPS data. In this case the desired coverage was 96% (b), the estimated coverage was 80% (c), and the achieved coverage was 67% (d). When sonar seabed coverage is for a safety critical task such as mine counter-measures (MCM), this represents an unacceptably large discrepancy between the acceptable risk (b), the perceived risk (c), and the actual risk (d) associated with assets and personnel transiting over this seabed area.

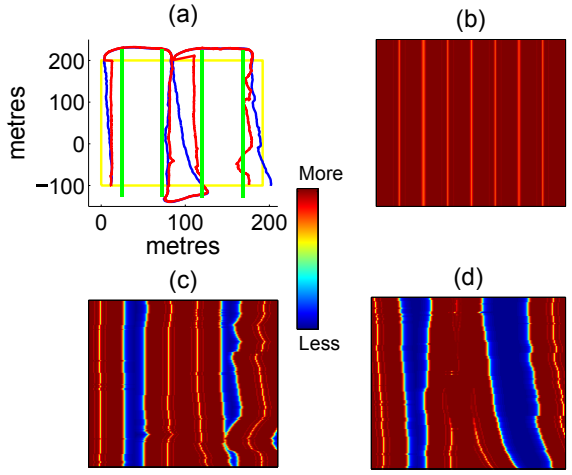

Fig. 1. **(a)** Plot of workspace to be covered (yellow) with desired tracks (green), estimated path (red), and actual path (blue); **(b)** desired coverage; **(c)** estimated coverage from EKF, and **(d)** actual coverage based on GPS data.

The actual AUV path can deviate from the planned path because: 1) the vehicle has insufficient command authority to follow the path, 2) external disturbances such as currents

*This work was supported by National Science and Engineering Research Council of Canada and Defense Research and Development Canada

[1]Computer Science and AI Lab at Massachusetts Institute of Technology in Cambridge, Massachusetts, USA lpaull@mit.edu

[2]Mine and Harbour Defense Group, Defense R&D Canada in Dartmouth, Nova Scotia, Canada mae.seto@drdc-rddc.gc.ca

[3]Collaborative Based Robotics and Automation (COBRA) group in the Department of Electrical and Computer Engineering at the University of New Brunswick, Fredericton, New Brunswick Canada howard@unb.ca

or sea states cause deviations, or 3) the AUV location estimate contains uncertainties and errors as a result of noisy sensor data. Path tracking errors have been considered in the general start-to-goal path planning literature (e.g. [6], [7], [8]), however, to a lesser extent in a coverage context. In [9], a heuristic method combines three types of behaviors: inward spiral, shifting spiral, and greedy. The application is a car-like robot that mows grass and the robot's kinematic constraints are explicitly considered. The coverage map is maintained and after the initial pass with inward spiral and shifting spiral behaviors, the missing areas are covered using a greedy approach. Localization uncertainty is accounted for by explicitly planning paths to have overlap across neighbouring sensor swaths.

In [10] a "probably approximately correct" measure of coverage performance is developed to account for sensor uncertainty. The authors correctly argue that once vehicle localization error is significant, the definition of complete coverage must be adapted to become probabilistic. For example, "80% certainty that at least 90% of the workspace has been covered" could be a valid mission objective, whereas "cover at least 85% of the workspace" is not. However, the approach in [10] only considers uniform sensor characteristics and provides no adaptive approach to account for the robot's pose uncertainty. Also, in [10] it is assumed that the localization error variance attains a steady-state. This is not a valid assumption for a dead-reckoning vehicle.

In general, the methods in the literature propose adjusting existing heuristics so that the vehicle uncertainty may be accounted for (e.g. move tracks or spirals closer together). However this can produce paths with unnecessary sensor overlap in the case that path tracking error is low. Here, we maintain the probability of coverage over the discretized workspace by projecting the location estimate through the coverage sensor characteristic. This approach has the distinct advantage that we can now use the probability of coverage over the workspace to plan paths for coverage that adaptively account for the sensor location uncertainty. We propose that an entropy reduction approach is appropriate for planning these paths.

The probabilistic coverage framework is generally applicable but particularly suited to the AUV seabed surveying mission.

To summarize, the contributions of the presented work are as follows:

1) A probabilistic coverage model that fuses state estimation with a sensor coverage model to obtain a stochastic representation of the coverage over the workspace.
2) A coverage path planning algorithm based on the probabilistic coverage representation that adaptively accounts for robot location uncertainty. Coverage is posed as an entropy reduction problem and paths are planned to meet this objective.
3) An application with in-water results of an AUV deployed for underwater seabed surveying for MCM.

The probabilistic coverage framework is developed in general terms in Sec. II. This framework is then applied to the AUV seabed surveying problem in Sec. III with development of the information-based path planner in Sec. IV. In-water results are presented in Sec. V and finally the paper concludes in Sec. VI.

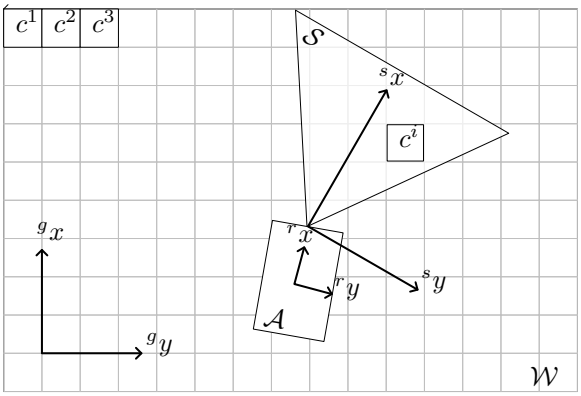

Fig. 2. Workspace $\mathcal{W}$ is decomposed into cells. As the robot, $\mathcal{A}$, moves, $\mathcal{W}$ becomes covered in a manner consistent with the coverage sensor geometry $\mathcal{S}$.

II. The Probabilistic Coverage Framework

We first formulate the area coverage problem with known poses. We then extend the formulation to consider uncertain poses and describe how to recursively update the probabilistic coverage map. Finally, we formally define new criteria for mission completion in the probabilistic case.

A. Area Coverage Problem Formulation

Consider a robot with platform geometry $\mathcal{A}$ and coverage sensor swath $\mathcal{S}$ (Fig. 2). Define the workspace, $\mathcal{W}$, as the area that is to be covered by the sensor.

The workspace is decomposed into N small grid cells where the size of the cells is sufficiently small that the coverage can be treated as uniform over the cell. Each cell is represented by its position in the workspace. For example, for the two-dimensional case, $\mathbf{c}^i \triangleq [x^i, y^i]^T$ such that x^i and y^i are the x and y locations, respectively, of cell $\mathbf{c}^i$ in the global frame[1].

If the robot takes a sensor measurement at time t, then the set of all cells that are somewhat covered by the measurement defines the coverage sensor swath, $\mathcal{S}_t$.

The position of a cell i in the sensor frame is obtained by performing a transformation from the global to the sensor frame through the robot body frame:

$$ {}^s\mathbf{c}_t^i \triangleq [{}^s x_t^i, {}^s y_t^i]^T = {}^s_r\mathrm{T}\ {}^r_g\mathrm{T}_t\ {}^g\mathbf{c}^i = {}^s_g\mathrm{T}_t\ {}^g\mathbf{c}^i \qquad (1) $$

where ${}^s\mathbf{c}_t^i$ and ${}^g\mathbf{c}^i$ are the location of the cell in the sensor and the global frame respectively and ${}^b_a\mathrm{T}$ is a homogeneous transformation from frame a to frame b. In the absence of any specified frame assume the global frame.

We can associate with each cell a value w_t^i that represents the level to which cell $\mathbf{c}^i$ is covered at time t.

[1]General notational convention: bold face indicates vector variable. Capital letter indicates random variable. Preceding superscripts indicate frames. Proceeding superscripts indicate cell index. Proceeding subscripts indicate time.

Based on a detailed investigation of the coverage sensor, such as ESPRESSO [11] for the case of AUV seabed surveying (See Sec. III), the cell coverage values are updated according to:

$$w_t^i = \mathcal{H}({}^s\mathbf{c}_t^i), \tag{2}$$

where $\mathcal{H}({}^s\mathbf{c}^i)$ represents the coverage sensor model and defines how to update the coverage value of the cells based on their locations in the sensor frame.

If we assume a uniform coverage sensor, cells are either completely covered or not at all, and $w \in \{0.5, 1\}$ [2]. This means that each cell is either covered ($w = 1$) or not ($w = 0.5$). In this case we state the complete coverage objective as requiring

$$w_t^i = 1, \forall i = 1..N. \tag{3}$$

However, with some sensors, such as the SSS, the coverage sensor performance is not uniform and $w \in [0.5, 1]$. As a result, (3) can become difficult or impossible to achieve depending on the model. The mission is generally considered complete either when a proportion of cells, P_1, have been covered to a specified level w_{thresh}:

$$\frac{1}{N}\#\{i | i = 1..N, w_t^i > w_{thresh}\} > P_1, \tag{4}$$

where $\#\{\cdot\}$ is the cardinality operator on a set, or when we have achieved a desired average coverage, w_{avg}, over the entire workspace:

$$\frac{1}{N}\sum_{i=1}^{N} w_t^i > w_{avg}, \tag{5}$$

B. Coverage with Uncertain Poses

We now remove the assumption common to most coverage algorithms that the coverage sensor is deterministically localized. As a result, (4) and (5) are not sufficient criteria for mission completion because they do not encapsulate the uncertainty in the coverage induced by the uncertainty in robot pose.

The filtered posterior pose distribution at time t given all previous odometry and measurements is given by $bel(\mathbf{x}_t)$ [12]:

$$bel(\mathbf{x}_t) \triangleq p(\mathbf{x}_t | \mathbf{u}_{1:t}, \mathbf{z}_{1:t}, \mathbf{x}_0) \tag{6}$$

The state at time t is recursively estimated through an approximation of the Bayes' filter which operates in a predict-update cycle. Prediction is done through [12]:

$$\bar{bel}(\mathbf{x}_t) = \int p(\mathbf{x}_t | \mathbf{x}_{t-1}, \mathbf{u}_t) bel(\mathbf{x}_{t-1}) d\mathbf{x}_{t-1} \tag{7}$$

and update is given by:

$$bel(\mathbf{x}_t) = \eta p(\mathbf{z}_t | \mathbf{x}_t) \bar{bel}(\mathbf{x}_t). \tag{8}$$

The probabilistic process model $p(\mathbf{x}_t | \mathbf{x}_{t-1}, \mathbf{u}_t)$ incorporates the noise associated with transitioning from $\mathbf{x}_{t-1}$ to $\mathbf{x}_t$ and the measurement model $p(\mathbf{z}_t | \mathbf{x}_t)$ incorporates noise associated with sensor updates.

The pose belief at time t is used to generate a probability of coverage for all grid cells in the workspace. Now, instead of each cell having one value that represents its coverage, it has a distribution representing the probability of coverage to different levels. The position of cell i in the sensor frame is now uncertain and is represented by a random variable ${}^s\mathbf{C}_t^i$ whose distribution is calculated by mapping the position of the cell in the global frame through the uncertain transformation from global to sensor frame:

$$p({}^s\mathbf{C}_t^i = {}^s\mathbf{c}_t^i) = p({}^s_g\mathrm{T}_t \; {}^g\mathbf{c}^i = {}^s\mathbf{c}_t^i) \triangleq p({}^s\mathbf{c}_t^i) \tag{9}$$

is the probability that cell i sits at location ${}^s\mathbf{c}_t^i$ in the sensor frame at time t.

The uncertain location of the cell in the sensor frame results in an uncertain coverage. Consequently, the coverage is represented by a random variable W_t^i where $p(W_t^i = w)$ represents the probability that cell i is covered to a coverage level w at time t considering all past AUV states.

It is useful to define a random variable $\breve{W}_t^i$ that represents the probability that cell i is covered to a level w resulting from *only* the sensor measurements at time t.

C. Propagating Robot Pose Uncertainty to Coverage Distribution

In this section we describe the process for estimating the coverage distribution due to a single coverage sensor measurement from an uncertain location. The distribution $p(\breve{W}_t^i = w)$, can be determined by propagating the uncertain cell location in the sensor frame through the coverage sensor model, $\mathcal{H}$:

$$\breve{W}_t^i = \mathcal{H}({}^s\mathbf{C}_t^i). \tag{10}$$

The distribution of $\breve{W}_t^i$ can be found by mapping the random variable $\breve{W}_t^i$ through the function $\mathcal{H}$ by extending the method in [13] to higher dimensions:

$$p(\breve{W}_t^i = w_t^i) = \frac{p({}^s\mathbf{C}_t^i = {}^s\mathbf{c}_t^i[1])}{|(\nabla\mathcal{H})_{{}^s\mathbf{c}_t^i[1]}|} + ... + \frac{p({}^s\mathbf{C}_t^i = {}^s\mathbf{c}_t^i[n])}{|(\nabla\mathcal{H})_{{}^s\mathbf{c}_t^i[n]}|} \tag{11}$$

where ${}^s\mathbf{c}_t^i[1], ..., {}^s\mathbf{c}_t^i[n]$ are the n solutions found when solving $w_t^i = \mathcal{H}({}^s\mathbf{c}_t^i)$:

$$w_t^i = \mathcal{H}({}^s\mathbf{c}_t^i[1]) = ... = \mathcal{H}({}^s\mathbf{c}_t^i[n]) \tag{12}$$

and $|(\nabla\mathcal{H})_{\mathbf{c}}|$ is the magnitude of the gradient of $\mathcal{H}$ evaluated at $\mathbf{c}$.

Eq (11) provides an explicit method to evaluate the coverage distribution of each coverage grid cell from a single uncertain pose. $\mathcal{H}({}^s\mathbf{c}_t^i)$ is evaluated from the coverage sensor model (2). $p({}^s\mathbf{c}_t^i)$ is generated by mapping the cell location in the global frame through the uncertain transformation ${}^s_g\mathrm{T}_t$ defined in (1).

[2]For convenience and to unify coverage problems defined by actuation and detection we define not covered as $w = 0.5$ and covered as $w = 1$. If the coverage sensor model is defined over [0,1] we can easily map it to the range [0.5,1]

Algorithm 1 Iterative coverage distribution estimation

$p(W_0^i = 0.5) = 1 \; \forall i = 1...N$
$bel(\mathbf{x}_0) \leftarrow$ distribution of prior pose state estimate
$t \leftarrow 1$
repeat
  $\bar{bel}(\mathbf{x}_t) = \int p(\mathbf{x}_t|\mathbf{x}_{t-1}, \mathbf{u}_t) bel(\mathbf{x}_{t-1}) d\mathbf{x}_{t-1}$
  $bel(\mathbf{x}_t) = \eta p(\mathbf{z}_t|\mathbf{x}_t) \bar{bel}(\mathbf{x}_t)$
  for all i such that $\mathbf{c}_i \in \mathcal{S}'_t$ **do**
    $p({}^s\mathbf{c}_t^i) = p({}^s_g\mathrm{T}_t \; {}^g\mathbf{c}_t^i = {}^s\mathbf{c})$
    $p(\breve{W}_t^i = w) = \int p(\breve{W}_t^i = w|{}^s\mathbf{C}_t^i = {}^s\mathbf{c}_t^i) p({}^s\mathbf{C}_t^i = {}^s\mathbf{c}_t^i) d{}^s\mathbf{c}_t^i$
    $p(W_t^i = w) = p(\breve{W}_t^i = w) \int_0^w p(W_{t-1}^i = \epsilon) d\epsilon + p(W_{t-1}^i = w) \int_0^w p(\breve{W}_t^i = \epsilon) d\epsilon$
  end for
  $t \leftarrow t + 1$
until mission completion

D. Recursive Coverage Estimation

Equation (11) provides a means to propagate the AUV pose uncertainty through the sensor characteristic to obtain an estimate of the coverage distribution from a single sensor pose. Over the course of a coverage mission, the AUV will move around the workspace and may cover cells multiple times. A means is needed to combine the coverage distribution from time t with all previous coverage instances at the same location from times 0 to $t-1$.

It is motivated in [4] and [12] that the most pessimistic way to fuse measurements of the same location, but at different times, is to assume that they are statistically dependent, in which case the maximum function is applied (the coverage can be no less than the greatest value it was covered to in all of the previous passes). Furthermore, it is argued that subsequent SSS measurements of one location for an MCM mission are statistically dependent in [14].

Using the statistical dependance assumption, we can recursively define the coverage distribution using the maximum function on random variables:

$$W_t^i = \max(\breve{W}_t^i, W_{t-1}^i) \tag{13}$$

where the distribution of W_t^i can be determined using [13]:

$$\begin{aligned} p(W_t^i = w) = p(\breve{W}_t^i = w) \int_0^w p(W_{t-1}^i = \epsilon) d\epsilon \\ + p(W_{t-1}^i = w) \int_0^w p(\breve{W}_t^i = \epsilon) d\epsilon \end{aligned} \tag{14}$$

As a result, the coverage distribution at time t for cell i is based only on the pose at time t (used to generate $\breve{W}_t^i$) and the coverage distribution at time $t-1$, W_{t-1}^i. As a result, the Markov assumption can be applied to the coverage sensor measurements and sensor data can be discarded once the coverage distribution at time t has been updated. An overview of the iterative coverage estimation process is summarized in Algorithm 1.

E. Full Trajectory Estimation for Coverage

This framework as proposed thus far is independent of the type of state estimation algorithm used. Coverage over the workspace is dependent on the entire sensor trajectory, therefore to obtain the best estimate of the coverage belief, we require the best estimate of the entire vehicle trajectory as opposed to just the present state. We update (6) to estimate the posterior of the entire vehicle trajectory:

$$bel(\mathbf{x}_{1:t}) \triangleq p(\mathbf{x}_t|\mathbf{u}_{1:t}, \mathbf{z}_{1:t}, \mathbf{x}_0). \tag{15}$$

This approach is particularly applicable to the case when a vehicle is receiving intermittent global position updates such as an AUV surfacing for GPS fixes. Each time the vehicle receives a global update, the trajectory is re-optimized and the coverage map is recalculated based on the updated state beliefs. In practice, a sliding window approach can be used to maintain constant time scalability.

F. New Definition of Mission Completion

As argued previously, the deterministic mission completion criteria (4) and (5) must now be updated to reflect the fact that the coverage is probabilistic.

The first completion criterion (4) requires that a proportion P_1 of the area be covered up to at least level w_{thresh}. This is updated to require that the proportion, P_1, of the area has a probability of being covered to at least a level w_{thresh} of at least P_2:

$$\frac{1}{N} \#\{i|p(W_t^i \geq w_{thresh}) \geq P_2, i = 1..N\} > P_1. \tag{16}$$

The second mission criterion criterion (5) is to have achieved a desired average coverage, w_{avg}, over the entire workspace. This is updated to require an expected average coverage greater than w_{avg}

$$\frac{1}{N} \sum_{i=1}^{N} E[W_t^i] = E[\frac{1}{N} \sum_{i=1}^{N} W^i] > w_{avg}. \tag{17}$$

In the case where the coverage sensor characteristic is uniform, $P_2 = 1$ and (16) reduces to the "probably approximately complete" measure of completeness presented in [10].

III. Applying the Probabilistic Coverage Framework to AUV Seabed Surveying

Some underwater seabed survey missions use sidescan sonar as the payload sensor. The SSS processes high frequency sonar echoes to generate an image of the seabed. An object on the seabed will cast a sonar shadow that can be analyzed to determine if it is potentially a mine. The onboard SSS gathers data as the AUV transits along rectilinear paths as shown in Fig. 3.

In 2006, the NATO Undersea Research Centre (now Centre for Marine Research and Experimentation) created a model to quantify minehunting sonar performance that incorporates physical parameters that influence the probability of detecting a target in sonar data called the Extensible Performance and Evaluation Suite for Sonar (ESPRESSO) [11], [15].

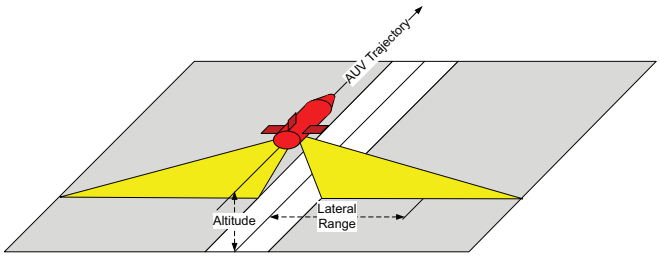

Fig. 3. An example of the AUV trajectory and corresponding area covered by its SSS.

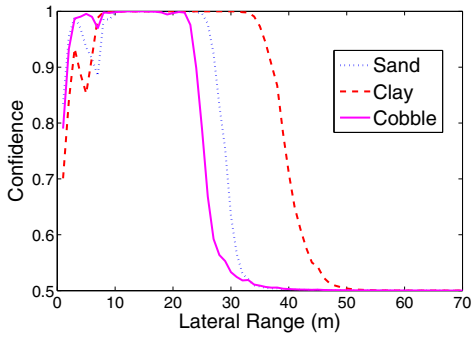

Fig. 4. Three sample lateral range $P(y)$ curves generated by ESPRESSO [11]. The AUV is equipped with sonar sensors on both sides of the vehicle, the plot shows only one side.

The output of the model is a lateral range curve, $P(y)$, that defines the probability that a target at lateral distance y from the AUV's track will be detected along that track and subsequently correctly classified as being suggestive of a mine (referred to as confidence). Parameters that affect the lateral range curve fall into four general categories: environmental, target, sonar, and platform (AUV).

Fig. 4 shows the lateral range curves generated by ESPRESSO for three different seabed types: cobble, sand, and clay, all at a water depth of 10 m.

Localization error is not negligible in AUV surveys since the AUV has no access to a global position reference when it is submerged. It is in this mode that the iterative coverage estimation process described by Algorithm 1 is performed.

Since the SSS can only generate useful mosaicked data when the AUV is in rectilinear motion, we simplify the problem by only considering the cross-track uncertainty in the AUV location. As a result, the pose distribution is projected onto the line orthogonal to the direction of AUV travel as shown in Fig. 5.

It is assumed that DVL, GPS, and compass noise are normally distributed (for a deeper investigation on the noise characteristics of these sensors and the Gaussian assumption see [16]) so that the AUV position is estimated as a bivariate Gaussian distribution of the random variables (X_t, Y_t):

$$\begin{bmatrix} x_t \\ y_t \end{bmatrix} \sim \mathcal{N}\left(\begin{bmatrix} \mu_{x_t} \\ \mu_{y_t} \end{bmatrix}, \begin{bmatrix} \sigma^2_{x_t x_t} & \rho_t \sigma_{x_t x_t} \sigma_{y_t y_t} \\ \rho_t \sigma_{x_t x_t} \sigma_{y_t y_t} & \sigma^2_{y_t y_t} \end{bmatrix} \right) \quad (18)$$

where ρ_t is the bivariate correlation coefficient between X_t and Y_t, μ values are means and σ values are covariances.

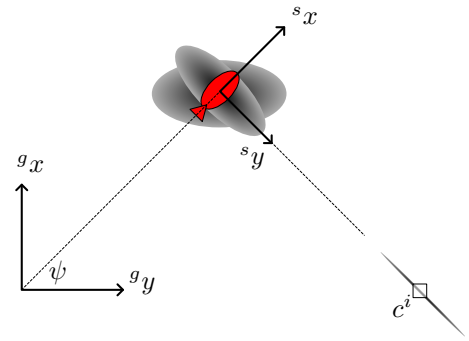

Fig. 5. Projection of 2D position distribution onto 1D line orthogonal to AUV motion.

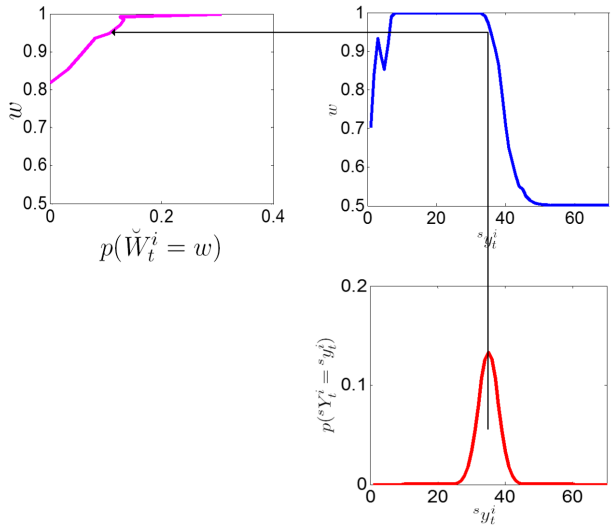

Fig. 6. The distribution of the cell in the sensor frame (bottom right) is mapped through the $P(y)$ curve (top right) to obtain a coverage distribution (top left).

The cell location in the global frame is transformed through ${}^s_g T_t$ into a distribution in the sensor frame $p({}^s\mathbf{C}_t^i = {}^s\mathbf{c}_t^i)$ and then the along-track (direction of ${}^s x_t^i$) uncertainty is marginalized out to yield a distribution for cell i in the cross-track direction: $p({}^s Y_t^i = {}^s y_t^i) \sim \mathcal{N}(\mu_{{}^s y_t^i}, \sigma^2_{{}^s y_t^i {}^s y_t^i})$ with:

$$\mu_{{}^s y_t^i} = (x^i - \mu_{x_t}) \sin\psi_t + (y^i - \mu_{y_t}) \cos\psi_t, \quad (19)$$

and:

$$\sigma_{{}^s y_t^i {}^s y_t^i} = \sigma^2_{x_t x_t} \sin^2\psi_t + \rho_t \sigma_{x_t x_t} \sigma_{y_t y_t} \sin 2\psi_t + \sigma^2_{y_t y_t} \cos^2\psi_t, \quad (20)$$

The coverage sensor model, $\mathcal{H}$, originally defined in (2) is now given by the lateral range characteristic, P:

$$\breve{W}_t^i = \mathcal{H}({}^s\mathbf{C}_t^i) = P({}^s Y_t^i). \quad (21)$$

Fig. 6 shows how the distribution of $\breve{W}_t^i$ is generated by mapping an uncertain cell location through the sensor characteristic. The distribution of the orthogonal distance of the cell from the sensor is shown in red (bottom right). The sonar coverage sensor model (ESPRESSO) is shown in blue (top right). The cell location distribution is mapped through the coverage sensor model to obtain the coverage distribution resulting from this one single measurement (top left).

A lower bound on the coverage can be obtained recursively by applying the maximum function on random variables defined in (14) to determine the coverage distribution W_t^i. Each time the vehicle surfaces for GPS, the trajectory is re-optimized and the coverage distributions are recalculated in a batch process. In practice there is no need to re-optimize the entire vehicle trajectory, only the parts that are still being appreciably changed by new GPS updates.

IV. Coverage Path Planning Within the Probabilistic Framework

Past approaches to AUV seabed surveying have planned structured (lawn mower or zig-zag) paths off-line and assumed that the tracks are followed exactly. We propose an information-based approach which extends our previous work [4] by accounting for uncertainty in the AUV pose.

A. The Confidence Map

Define a binary random variable $\breve{T}_t^i \in \{0, 1\}$ that represents whether cell $\mathbf{c}^i$ will be correctly classified as either containing a mine, or not, at time t:

$$\begin{aligned} p(\breve{T}_t^i = 1) &= p(\text{detection}) + p(\text{correct no detection}) \\ p(\breve{T}_t^i = 0) &= p(\text{false alarm}) + p(\text{missed target}) \end{aligned} \tag{22}$$

For each $\breve{T}_t^i$, $p(\breve{T}_t^i = 1) \in [0.5, 1]$ represents the confidence, or probability of correct classification, of cell $\mathbf{c}^i$ as either containing a target or not, and $p(\breve{T}_t^i = 0) = 1 - p(T_t^i = 1)$ is the probability of incorrect classification.

Additionally, for each cell, i, associate a binary random variable, T_t^i, where $p(T_t^i = 1)$ represents the confidence by combining all the "looks" of cell i from the start of the survey until time t. This collection of random variables, $T_t^{1:N}$ is the confidence map.

At the start of the mission the confidence values are all initialized to 0.5: $p(T_{t_0}^i = 1) = 0.5,\ \forall i = 1..N$.

B. Updating the Confidence Map

As the AUV navigates around the workspace the confidence map is updated based on the current AUV pose and the parameters that affect sonar performance: environment, target, sonar, and platform.

The target detection event can be represented by the Bayes' network shown in Fig. 7. Any variable with the superscript i varies across the workspace and any variable with the subscript t varies with time.

Define $\boldsymbol{\mathcal{E}}_t^i = \{\mathbf{E}^i, \mathbf{S}, \mathbf{F}, \mathbf{V}_t\}$ as the set of all random variables that affect the generation of the lateral range characteristic at cell i and time t. We can express the joint probability of confidence based on a single observation and combination of sensor, environment, and AUV pose as:

$$p(\breve{T}_t^i = 1 | \boldsymbol{\mathcal{E}}_t^i = \boldsymbol{\varepsilon}_t^i, \mathbf{X}_t = \mathbf{x}_t) p(\boldsymbol{\mathcal{E}}_t^i = \boldsymbol{\varepsilon}_t^i) p(\mathbf{X}_t = \mathbf{x}_t) \tag{23}$$

Denote the sonar lateral range characteristic generated by the ESPRESSO model with parameters $\boldsymbol{\varepsilon}_t^i$ as $P_{\boldsymbol{\varepsilon}_t^i}(y)$ where

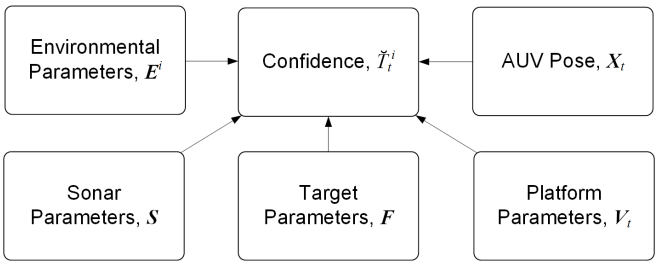

Fig. 7. Bayes' network representing target detection similar to [17]. Arrows represent conditional probabilities.

y is the lateral range. $p(\breve{T}_t^i = 1 | \boldsymbol{\mathcal{E}}_t^i = \boldsymbol{\varepsilon}_t^i, \mathbf{X}_t = \mathbf{x}_t)$ is read directly from the lateral range curve:

$$p(\breve{T}_t^i = 1 | \boldsymbol{\mathcal{E}}_t^i = \boldsymbol{\varepsilon}_t^i, \mathbf{X}_t = \mathbf{x}_t) = \begin{cases} P_{\boldsymbol{\varepsilon}_t^i}({}^s y_t^i) & \text{if } \mathbf{c}^i \in \mathcal{S}_t \\ 0.5 & \text{otherwise} \end{cases} \tag{24}$$

where ${}^s y_t^i$ is the orthogonal distance from the AUV track to the cell i at time t. For simplicity of formulation, we assume here that the environmental parameters $\boldsymbol{\mathcal{E}}_t^i$ are known ($p(\boldsymbol{\mathcal{E}}_t^i = \boldsymbol{\varepsilon}_t^i) = 1$) however the extension to the case where both the environmental parameters and pose are uncertain is straightforward. For a more detailed investigation of the case of uncertain parameters see [4].

We can evaluate the confidence resulting from a single sonar sensor measurement at time t for cell i by marginalizing over all poses:

$$\begin{aligned} p(\breve{T}_t^i = 1) &= \sum_{\mathbf{x}_t} p(\breve{T}_t^i = 1, \boldsymbol{\mathcal{E}}_t^i = \boldsymbol{\varepsilon}_t^i, \mathbf{X}_t = \mathbf{x}_t) \\ &= E_{\mathbf{X}_t}[p(\breve{T}_t^i = 1 | \boldsymbol{\mathcal{E}}_t^i = \boldsymbol{\varepsilon}_t^i, \mathbf{X}_t = \mathbf{x}_t)] \\ &= \begin{cases} E_{{}^s Y_t^i}[P_{\boldsymbol{\varepsilon}_t^i}({}^s Y_t^i)] & \text{if cell } c^i \in \mathcal{S}_t \\ 0.5 & \text{otherwise} \end{cases} \end{aligned} \tag{25}$$

The sonar lateral range curve is a specific example of the general coverage sensor function $\mathcal{H}$ defined in (2). So (25) can be rewritten using the general framework of Sec. II as:

$$E_{{}^s Y_t^i}[P_{\boldsymbol{\varepsilon}_t^i}({}^s Y_t^i)] = E_{{}^s \mathbf{C}_t^i}[\mathcal{H}({}^s \mathbf{C}_t^i)] = E[\breve{W}_t^i]. \tag{26}$$

Consequently, the confidence from one look $p(\breve{T}_t^i = 1)$ in the case of the AUV seabed coverage problem is evaluated as the mean of the coverage distribution from the probabilistic framework. For the cells that are in the sensor swath:

$$p(\breve{T}_t^i = 1) = E[\breve{W}_t^i] \tag{27}$$

The final confidence after combining n looks can be expressed as:

$$p(T_t^i = 1) = E[W_t^i] = E[\max\{\breve{W}_{t_1}^i, \breve{W}_{t_2}^i, ..., \breve{W}_{t_n}^i\}] \tag{28}$$

where the necessity to maintain the entire coverage distributions as opposed to just the distribution means is due to the fact that the expectation operator, E, cannot be distributed across the maximum operator: $E[\max\{\breve{W}_{t_1}^i, \breve{W}_{t_2}^i\} \neq \max\{E[\breve{W}_{t_1}^i], E[\breve{W}_{t_2}^i]\}$.

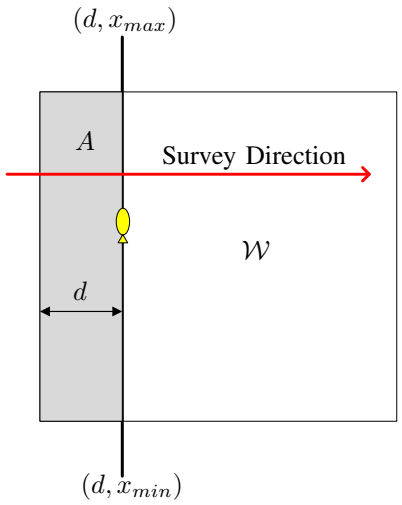

Fig. 8. The value of d should be optimized such that the portion of the map defined by A satisfies the mission completion criterion

C. Information-Based Coverage Path Planning

It is proposed here that Shannon entropy reduction of the confidence map variables is an appropriate and novel way of adaptively achieving coverage. The expected entropy reduction (EER) is given by:

$$\Delta H(T_t^i|\boldsymbol{\mathcal{E}}_t^i, \mathbf{X}_t) \triangleq H(T_t^i) - E_{\boldsymbol{X}_t}[H(T_t^i|\boldsymbol{\mathcal{E}}_t^i, \mathbf{X}_t)], \quad (29)$$

where $H(T) = -E[\log p(T)]$ is the Shannon entropy. The EER defines a scalar quantity that represents the *a priori* expected amount of information that will be gained about T_t^i by making the sonar measurement from the uncertain pose $\mathbf{X}_t$ at time t with environmental parameters $\boldsymbol{\mathcal{E}}_t^i$.

The EERs specify a way of combining the potential benefits of sensor observations additively. We can compute the total EER at time t as the sum of the EERs of every cell in the sensor swath:

$$\Delta H(\mathbf{T}_t|\boldsymbol{\mathcal{E}}_t^{1:N}, \mathbf{X}_t) = \sum_{i:\mathbf{c}^i \in \mathcal{S}_t} \Delta H(T_t^i|\boldsymbol{\mathcal{E}}_t^i, \mathbf{X}_t) \quad (30)$$

where $\mathbf{T}_t \triangleq [T_t^1, T_t^2, ..., T_t^N]$.

In order to plan a path, we perform a search over a set of potential next poses and evaluate their benefit. In this flexible framework we can specify any meaningful domain of next poses to be searched over in order to find a locally optimal path. Here we propose one possible domain that is particularly well-suited to the seabed surveying application. We optimize the location of each subsequent track after each previous track is completed. The placement of the next track to be followed should maximize the information to be gained subject to the constraint that no gaps are left to guarantee actual coverage in the field.

From Fig. 8, the optimization takes place over the domain of d subject to the constraint that the area A satisfy mission completion. Define the next track as τ_d parameterized by s:

$$\begin{aligned} &\tau_d : [0,1] \rightarrow Q_{free}, s \rightarrow \tau_d(s) \\ &\quad \tau_d(0) = (d, x_{min});\ \tau_d(1) = (d, x_{max}) \end{aligned} \quad (31)$$

where x_{min} and x_{max} are the minimum and maximum x values of the track, and Q_{free} is the free configuration space, or set of all possible poses in the environment that will not collide with obstacles [18].

In this case we select (17), which is the probabilistic version of (5), as the criterion for mission completion since average confidence is an accurate representation of the risk associated with moving an asset and personnel over the area. The average confidence objective is used and motivated in other work on AUV MCM, such as [14].

The optimization to select the value d that maximizes the information gained is:

$$B(d) \triangleq \int_0^1 \Delta H(\mathbf{T}_t|\boldsymbol{\mathcal{E}}_t^{1:N}, \tau_d(s))ds \quad (32)$$

subject to the constraint:

$$\frac{1}{A}\sum_{i:\mathbf{c}^i \in A}^{N} E[W_t^i] = \frac{1}{A}\sum_{i:\mathbf{c}^i \in A}^{N} p(T_t^i) = 1 > w_{avg} \quad (33)$$

V. In-Water Results

In-water tests were performed to test the proposed methods. Example results are shown in Fig. 9 and Fig. 10. This was performed in the same workspace as Fig. 1, which is a square box approximately 200m by 300m. The AUV runs on the surface but the GPS data is not fused into the state estimate unless the AUV is at the beginning or end of a track (where a GPS fix might normally occur). Each time a track is completed, the optimization (32) is re-run until convergence. In some cases acquiring the GPS fix and computing the optimal track takes time, so the AUV executes a loiter pattern while this is ongoing. The mission completion criterion is:

$$\frac{1}{N}\sum_{i=1}^{N} E[W_t^i] = \frac{1}{A}\sum_{i:\mathbf{c}^i \in A}^{N} p(T_t^i) = 1 > 0.985 \quad (34)$$

or a mean average probability of 98.5% coverage.

The final trajectory and achieved coverage map from the GPS data are shown in Fig. 10, where the blue dot indicates the moment at which the coverage objective was met. The essential new capability here is that even though the AUV has very poor path tracking capability, it is still able to achieve its coverage objective.

VI. Concluding Remarks

This paper presents a probabilistic framework within which paths can be generated that guarantee coverage based on new probabilistic coverage criteria. The pose belief is used to generate a coverage estimate that is maintained as the robot navigates around its workspace. This is applied to the example of autonomous underwater vehicle seabed coverage for mine counter-measures. A path planning framework within the probabilistic coverage space is proposed based on information theory. It is shown that with this adaptive approach it can be guaranteed that mission coverage objectives are met.

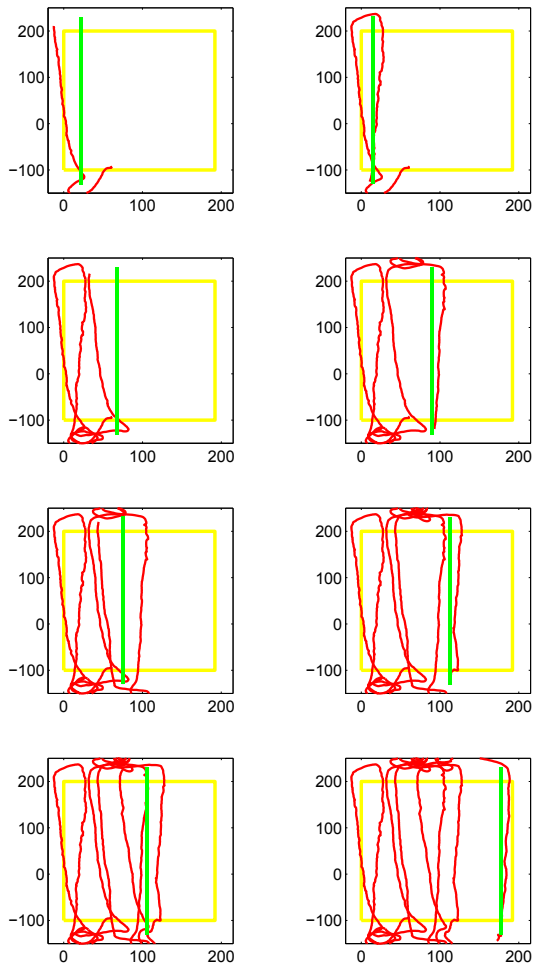

Fig. 9. The 8 plots show the state of the system after GPS updates are obtained nearing the end of each track. Time progresses from left to right and top to bottom. Units are in meters. The sensor characteristic used is the 10m depth cobble seabed type of Fig. 5. In each plot: **yellow**: workspace to be covered; **green**: track that has just been followed, and **red**: achieved trajectory that has been followed to that point based on the GPS data. Each time a track is finished the location of the next track is optimized based on (34) so that the workspace is guaranteed to be covered. The AUV is able to cover the area to 98.9% even though it is drifting more than 20m over a 200m track.

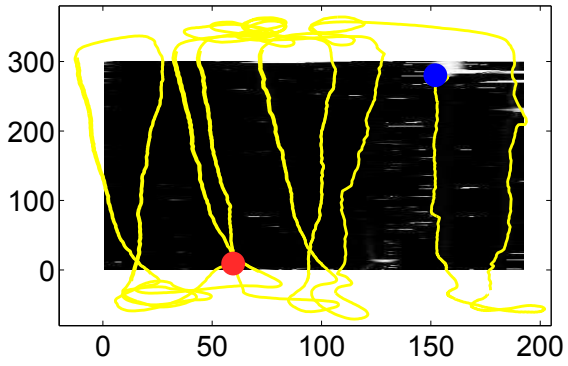

Fig. 10. The final estimated trajectory overlaid on the coverage map (darker area indicates higher coverage). Final mean confidence is 98.9% and required 9 tracks to complete.

This is the first known method that explicitly accounts for robot uncertainty for area coverage and a path planning approach is presented that exploits this probabilistic representation to achieve coverage even in the case that localization is poor.

In the case of a safety critical application such as AUV MCM, it is motivated that having the most accurate estimate possible of the state of the coverage over the workspace is important, since overconfidence or missed areas are especially undesirable.

References

[1] Ercan U. Acar and Howie Choset, "Sensor-based coverage of unknown environments: Incremental construction of Morse decompositions," *International Journal of Robotics Research*, vol. 21, pp. 345–367, 2002.

[2] Ercan U. Acar, Howie Choset, Yangang Zhang, and Mark J. Schervish, "Path planning for robotic demining: Robust sensor-based coverage of unstructured environments and probabilistic methods," *I. J. Robotic Res.*, vol. 22, no. 7-8, pp. 441–466, 2003.

[3] Howie Choset, "Coverage of known spaces: the Boustrophedon cellular decomposition," *Autonomous Robots*, vol. 9, pp. 247–253, 2000.

[4] L. Paull, S. Saeedi, M. Seto, and H. Li, "Sensor-driven online coverage planning for autonomous underwater vehicles," *Mechatronics, IEEE/ASME Transactions on*, vol. 18, no. 6, pp. 1827–1838, Dec 2013.

[5] L. Paull, S. Saeedi, M. Seto, and H. Li, "AUV navigation and localization: A review," *Oceanic Engineering, IEEE Journal of*, vol. 39, no. 1, pp. 131–149, Jan. 2014.

[6] Alain Lambert and Nadine Le Fort-Piat, "Safe task planning integrating uncertainties and local maps federations," *I. J. Robotic Res.*, vol. 19, no. 6, pp. 597–611, 2000.

[7] Samuel Prentice and Nicholas Roy, "The belief roadmap: Efficient planning in belief space by factoring the covariance," *The International Journal of Robotics Research*, vol. 28, no. 11-12, pp. 1448–1465, 2009.

[8] L. Blackmore, M. Ono, and B.C. Williams, "Chance-constrained optimal path planning with obstacles," *Robotics, IEEE Transactions on*, vol. 27, no. 6, pp. 1080–1094, dec. 2011.

[9] M. Bosse, N. Nourani-Vatani, and J. Roberts, "Coverage algorithms for an under-actuated car-like vehicle in an uncertain environment," in *Robotics and Automation, 2007 IEEE International Conference on*, april 2007, pp. 698–703.

[10] Colin Das, Aaron Becker, and Timothy Bretl, "Probably approximately correct coverage for robots with uncertainty," in *Intelligent Robots and Systems (IROS), 2011 IEEE/RSJ International Conference on*, sept. 2011, pp. 1160–1166.

[11] G. Davies and E. Signell, "ESPRESSO scientific user guide," NURC-SP-2006-003, NATO Underwater Research Centre, 2006.

[12] Sebastian Thrun, Wolfram Burgard, and Dieter Fox, *Probabilistic Robotics*, The MIT press, Cambridge, Massachusetts, USA, 2005.

[13] Athanasios Papoulis and S. Unnikrishna Pillai, *Probability, Random Variables and Stochastic Processes*, McGraw Hill, fourth edition, 2002.

[14] D.P. Williams, "On optimal AUV track-spacing for underwater mine detection," in *Robotics and Automation (ICRA), 2010 IEEE International Conference on*, May 2010, pp. 4755–4762.

[15] V. Myers and M. Pinto, "Bounding the performance of sidescan sonar automatic target recognition algorithms using information theory," *IET Radar Sonar Navig.*, vol. 1, no. 4, pp. 266–273, 2007.

[16] Sarah E Webster, Ryan M Eustice, Hanumant Singh, and Louis L Whitcomb, "Advances in single-beacon one-way-travel-time acoustic navigation for underwater vehicles," *The International Journal of Robotics Research*, vol. 31, no. 8, pp. 935–950, 2012.

[17] Cheghui Cai and Silvia Ferrari, "Information-driven sensor path planning by approximate cell decomposition," *IEEE Transactions on Systems, Man, and Cybernetics - Part B: Cybernetics*, vol. 39, no. 3, pp. 672–689, June 2009.

[18] H. Choset, W. Burgard, S. Hutchinson, G. Kantor, L. E. Kavraki, K. Lynch, and S. Thrun, *Principles of robot motion: Theory, agorithms, and implementation*, MIT Press, June 2005.